Endocrine regulation of airway clearance in *Drosophila*

Do-Hyoung Kim[a,b], Young-Joon Kim[b], and Michael E. Adams[a,c,1]

[a]Department of Entomology, University of California, Riverside, CA 92521; [b]School of Life Sciences, Gwangju Institute of Science and Technology, 61005 Gwangju, South Korea; and [c]Department of Cell Biology & Neuroscience, University of California, Riverside, CA 92521

Edited by David L. Denlinger, Ohio State University, Columbus, OH, and approved January 5, 2018 (received for review October 5, 2017)

Fluid clearance from the respiratory system during developmental transitions is critically important for achieving optimal gas exchange in animals. During insect development from embryo to adult, airway clearance occurs episodically each time the molt is completed by performance of the ecdysis sequence, coordinated by a peptide-signaling cascade initiated by ecdysis-triggering hormone (ETH). We find that the neuropeptide Kinin (also known as Drosokinin or Leukokinin) is required for normal respiratory fluid clearance or "tracheal air-filling" in *Drosophila* larvae. Disruption of Kinin signaling leads to defective air-filling during all larval stages. Such defects are observed upon ablation or electrical silencing of *Kinin* neurons, as well as RNA silencing of the Kinin gene or the ETH receptor in *Kinin* neurons, indicating that ETH targets Kinin neurons to promote tracheal air-filling. A Kinin receptor mutant fly line (*Lkr*^{f02594}) also exhibits tracheal air-filling defects in all larval stages. Targeted Kinin receptor silencing in tracheal epithelial cells using *breathless* or *pickpocket* (*ppk*) drivers compromises tracheal air-filling. On the other hand, promotion of Kinin signaling in vivo through peptide injection or *Kinin* neuron activation through *Drosophila* TrpA1 (dTrpA1) expression induces premature tracheal collapse and air-filling. Moreover, direct exposure of tracheal epithelial cells in vitro to Kinin leads to calcium mobilization in tracheal epithelial cells. Our findings strongly implicate the neuropeptide Kinin as an important regulator of airway clearance via intracellular calcium mobilization in tracheal epithelial cells of *Drosophila*.

Kinin | ecdysis-triggering hormone | tracheal collapse | tracheal air-filling | *pickpocket*

Animals share similar complex respiratory organs consisting of highly branched, tubular epithelia for efficient gaseous exchange (1). At critical times during development, rapid clearance of fluid-filled airway passages becomes necessary to achieve optimal gas exchange across the respiratory epithelium. Such rapid airway clearance occurs at birth in mammals (2, 3) and episodically in the arthropod tracheal system at the end of each molt, immediately preceding the ecdysis behavioral sequence (EBS) that culminates in shedding of old cuticle (4, 5). During each molt, insects build a new tracheal network scaled to the larger size of the subsequent stage. Toward the end of the molt, this incipient airway network is filled with molting fluid. Completion of the molt occurs through tracheal air-filling and performance of the EBS following release of ecdysis triggering hormone (ETH). Air-filling of new trachea is preceded by collapse of the old trachea (5). Here we adopt the nomenclature suggested by Förster and Woods (4) to distinguish between tracheal inflation (filling of the tracheal tubes with fluid) and tracheal air-filling (replacement of liquid in the tracheal system with gas).

Previous studies of the *Drosophila* EBS showed that, within minutes of ETH release into the hemolymph, tracheal collapse and air-filling occur, followed shortly thereafter by initiation of preecdysis behavior (5, 6). Coincidentally, ETH targets *Kinin* neurons to mobilize intracellular calcium, leading to release of this peptide into the hemolymph (7). Kinin induces fictive preecdysis behavior in the isolated CNS of *Manduca*, and Kinin signaling is necessary for proper scheduling of preecdysis behavior in *Drosophila* (7, 8). Given the short latency between *Kinin* neuron activation and tracheal air-filling following ETH release (5), we hypothesized a functional role for Kinin in this vital physiological event. Kinin has been associated for many years with myotropic actions and promotion of ion and fluid transport (9–11). Furthermore, Kinin signaling is important in regulation of preecdysis behavior, confirming its involvement in early events during ecdysis (7, 8).

In both humans and fruit flies, the degenerin/epithelial Na^+ channel (DEG/ENaC) family encoded by *pickpocket* (*ppk*) genes is a primary ion channel mediating salt and liquid transport during airway clearance (12). In *Drosophila*, nine different *ppk* genes are expressed in the tracheal system and contribute to tracheal air-filling (12). *ppk* cells coexpress the transmembrane protein Wurst, which is essential for endocytosis during tracheal air-filling (13).

Because downstream signaling mechanisms underlying ETH-induced tracheal air-filling remain obscure, we undertook this study, the results of which strongly implicate Kinin in the signaling cascade responsible for tracheal air-filling during the EBS.

Results

Kinin Deficiency Leads to Loss of Tracheal Air-Filling. We generated *Kinin-GAL4* driver lines using a (~3.3 kb) promoter sequence upstream of the Kinin coding region (6, 14) and verified cell-specific expression in larval stages 1–3 by crossing *Kinin-GAL4* to *UAS-mCD8-GFP*, followed by double immunohistochemical staining with antisera directed against GFP and Kinin (Fig. S1). Three groups of Kinin-expressing neurons occur in the brain, subesophageal neuromeres, and abdominal neuromeres, consistent with previous reports (15, 16). We ablated *Kinin* neurons using the GAL4/UAS method for cell-specific expression of apoptosis genes *reaper* (*rpr*) and *head inversion defective* (*hid*) (17). Kinin-cell killing (CK) led to tracheal air-filling defects during all three larval instars; individuals were scored as complete or partial failure (Fig. 1). For example, during the first instar, 45% of *Kinin-GAL4 (3), UAS-rpr, UAS-hid* [*Kinin (3)>rpr, hid*] larvae exhibited complete failure, 33% showed partial failure, and 22% were normal. Doubling copy number of the *Kinin-GAL4* transgene [*Kinin (2, 3)>rpr, hid*] resulted in tracheal air-filling defects in all first-instar individuals sampled (78% complete and 22% partial failure). No air-filling defects were observed in control flies

Significance

The branched epithelial structure of the respiratory system, which is highly conserved in the animal kingdom, develops under liquid-filled conditions. In mammals at birth and insects at ecdysis, such respiratory networks undergo air-filling. We found that the neuropeptide Kinin promotes air-filling in the fruit fly respiratory system just prior to ecdysis by mobilizing calcium in tracheal epithelial pickpocket cells, which express homologs of mammalian epithelial Na^+ channels.

Author contributions: D.-H.K., Y.-J.K., and M.E.A. designed research; D.-H.K. and M.E.A. performed research; D.-H.K. and Y.-J.K. contributed new reagents/analytic tools; D.-H.K. and M.E.A. analyzed data; and D.-H.K., Y.-J.K., and M.E.A. wrote the paper.

The authors declare no conflict of interest.

This article is a PNAS Direct Submission.

[1]To whom correspondence should be addressed. Email: michael.adams@ucr.edu.

This article contains supporting information online at www.pnas.org/lookup/suppl/doi:10.1073/pnas.1717257115/-/DCSupplemental.

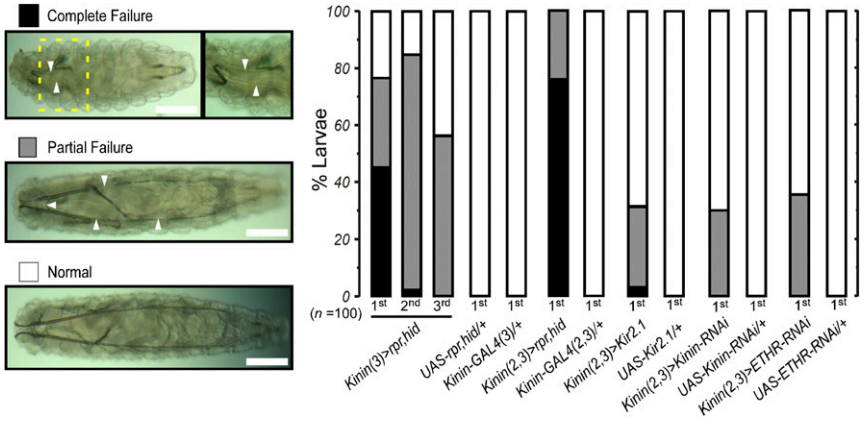

Fig. 1. Impairment of Kinin signaling leads to tracheal air-filling defects. Tracheal air-filling defects observed upon impairment of Kinin signaling through expression of apoptosis genes (*rpr, hid*), inward rectifier K^+ channel (Kir2.1), Kinin-RNAi, or ETH receptor-RNAi in *Kinin* neurons. Tracheal air-filling defects in flies were displayed as complete failure (black) when the tracheal system was entirely devoid of air or partial failure (gray bars). Doubling gene dosage through GAL4 expression on both second and third chromosomes [e.g., *Kinin (*2, 3)] caused more severe air-filling defects. Magnified image of the yellow dashed *Inset* box is shown *Right*. Arrowheads indicate the regions where failures of tracheal air-filling are observed. Larval stages examined are indicated below each bar. *UAS-Kinin-RNAi* and *UAS-ETHR-RNAi* carry *UAS-Dicer2*. (Scale bars, 100 μm.)

carrying either the *GAL4* or *UAS* transgene alone. Targeted ablation of *Kinin* neurons was confirmed by absence of *Kinin* cell labeling in Kinin-CK flies of all larval instars (Fig. S1 *B–D*).

We employed several additional strategies aimed at disrupting Kinin signaling, including electrical silencing via expression of an inward rectifier K^+ channel (Kir2.1), Kinin gene RNAi, and ETH receptor gene RNAi. Test animals showed tracheal air-filling defects in all cases, suggesting that a signaling cascade triggered by ETH is involved in tracheal air-filling mediated by Kinin signaling. Although severity of tracheal air-filling defects caused by Kir2.1 or RNAi is lower than that of Kinin CK flies, these flies showed low survival rates during development (Fig. S2*A*). For example, 68.6% of *Kinin (*2, 3*)>Kir2.1* flies showed normal tracheal air-filling during the first instar, but none survived to the prepupal stage (Fig. S2*B*). Low survival rate may be attributed to air-filling defects in fine tracheoles, disruption of ion and water balance (18), or ecdysis behavioral defects (7).

A Kinin Receptor Mutant Exhibits Tracheal Air-Filling Defects. Further evidence implicating Kinin signaling in tracheal air-filling comes from Kinin receptor mutant flies (Lkr^{f02594}) carrying a *piggyBac* insertion in exon 1 of the Kinin receptor gene (Fig. 2*A*). This *Lkr* mutant is a hypomorph, exhibiting ∼25% reduction in level of *Lkr* gene expression (7). Despite this rather marginal reduction, homozygous Lkr^{f02594} flies showed clear, partial tracheal air-filling defects (20–80%), although they were comparatively less severe than those observed in Kinin-CK flies (Fig. 2*B*).

To verify that this tracheal air-filling defect is a consequence of the insertional mutation in the Kinin receptor gene, Lkr^{f02594} was combined with deficiency lines *Df(3L)Exel6105* or *Df(3L)ZN47*, each of which carries a deletion that covers the Kinin receptor locus (Fig. 2 *B* and *C*). Total percentages of tracheal air-filling defects in transheterozygotes Lkr^{f02594}/*Df(3L)Exel6105* and Lkr^{f02594}/*Df(3L)ZN47* were 94.5% and 92.1%, respectively (Fig. 2*B*). In first-instar larvae, these defects are much more severe than that of

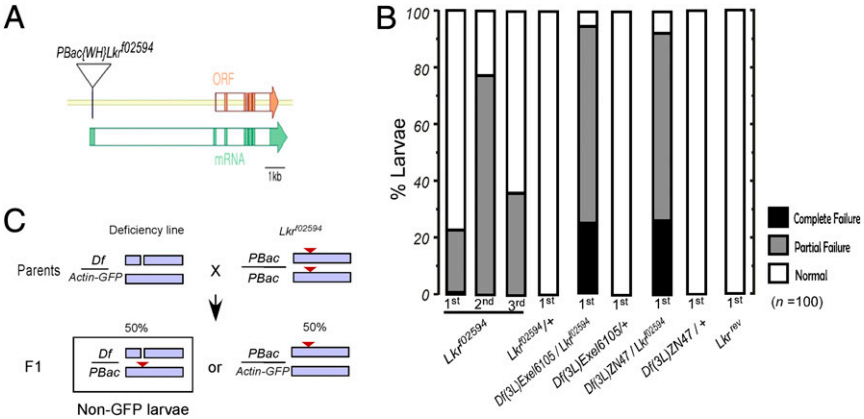

Fig. 2. Mutation of the Kinin receptor gene causes tracheal air-filling defects. (*A*) *PiggyBac* insertional mutant allele in the Kinin receptor locus (Lkr^{f02594}). Schematic drawing of the Kinin receptor gene structure in region 64E of chromosome *3L*; location of the *piggyBac* insertion in an upstream, untranslated exon is indicated. Green boxes are exons for the Kinin receptor gene. Orange boxes are ORFs. (*B*) Homozygous Kinin receptor mutant Lkr^{f02594} showed tracheal air-filling defects in all larval stages. Severity of defect was highly increased in complementation tests: 94.5% in Lkr^{f02594}/*Df(3L)Exel6105* and 92.1% in Lkr^{f02594}/*Df(3L)ZN47*. Precise excision of the piggyBac construct from Lkr^{f02594} generated a revertant allele Lkr^{rev}, rescuing the tracheal air-filling defect (see also Fig. S3). Larval stages observed are indicated below the bars. (*C*) Crossing scheme for the complementation test to confirms that the *piggyBac* insertion in Kinin receptor mutant causes tracheal air-filling defects. To aid recognition of Lkr^{f02594}/*Df* transheterozygous larvae, the chromosome with deficiency [*Df(3L)Exel6105* or *Df(3L)ZN47*] having deletion of the Kinin receptor gene was balanced with a sister chromosome carrying an *actin-GFP* transgene.

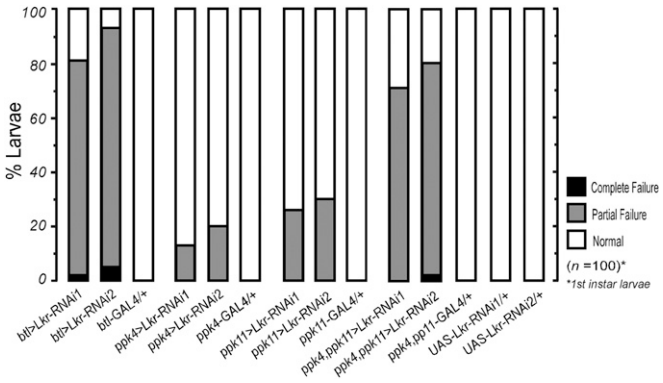

Fig. 3. ENaC family *ppk* cells in trachea engage in Kinin signaling for regulation of tracheal air-filling. Trachea-targeted *Kinin receptor* (*Lkr*)*-RNAi* expression using *breathless(btl)-GAL4* showed tracheal air-filling defects, implying presence of the kinin receptor in the tracheal system. Defects in tracheal air-filling following expression of *Lkr-RNAi* in *ppk* cells suggest that kinin signaling and ENaC may connected. GAL4 lines carry UAS-Dicer2. All data are taken from first-instar larvae.

the Lkr^{f02594} homozygote (22.6%), suggesting that the *piggyBac* insertion in the *Lkr* locus accounts for the tracheal air-filling defect.

Finally, we rescued the tracheal air-filling defect by precise excision of the *piggyBac* insertion by crossing Lkr^{f02594} with *piggyBac* transposase flies. Revertants produced from this cross (Lkr^{rev}) were completely devoid of tracheal air-filling defects (Fig. 2*B*). Precise excision of the *piggyBac* insertion was confirmed by paired PCR reactions and sequencing (Fig. S3).

Kinin Targets Tracheal Epithelial Cells for Airway Clearance. We hypothesized that Kinin mediates tracheal air-filling through activation of receptors expressed in tracheal epithelial cells. We therefore checked for abnormal air-filling phenotypes after silencing the Kinin receptor gene in all tracheal epithelial cells using the trachea-targeted *breathless (btl)-GAL4* driver (Fig. 3). More than 80% of *btl>Lkr-RNAi* individuals showed tracheal air-filling defects during the first larval instar. *Breathless-GAL4* has been reported to drive gene expression in the trachea (13, 19, 20), but recent reports show expression also in the glia (21). To check for possible glia-related air-filling phenotypes, we tested *Lkr* knockdown using the glial-specific driver *repo-GAL4*, and the neuro-glial driver *ELAV-GAL4*, which covers neurons and glia (22) (Fig. S4*A*). In both cases, we found no tracheal air-filling defects. To confirm the expression pattern of *btl-GAL4*, we checked for GFP-associated fluorescence in *btl>myr-GFP* flies and observed strong signals from tracheal tubules (Fig. S5). Brain and gut showed no evidence of GFP-associated fluorescence, except for that associated with tracheation. Malpighian tubules showed no GFP expression. Upon testing for tracheal air-filling phenotypes arising from Lkr knockdown using GAL4 drivers expressing pan-neuronally (*nSyb-GAL4*) (23), in the peripheral nervous system (*pebbled-GAL4*) (7), and in the gut (*NP3084-GAL4*) (24), we found no evidence for tracheal air-filling defects (Fig. S4*B*).

One possible consequence of Kinin receptor activation in tracheal epithelial cells is modulation of ENaC, known to be important for respiratory air-filling in both *Drosophila* and humans (12, 25). In *Drosophila*, ENaC channels are expressed in tracheal *ppk* cells. Expression of *Lkr-RNAi* using *ppk-GAL4* drivers led to tracheal air-filling defects (Fig. 3). Severity of phenotypes increased following use of doubly homozygous *ppk4-GAL4;ppk11-GAL4* (>70%). Expression of the Kinin receptor in tracheal epithelial cells was confirmed by staining *ppk4*, *ppk11>mCD8-EGFP* with anti-Lkr antibody (Fig. S6).

Kinin Mobilizes Calcium in *ppk*-Expressing Tracheal Epithelial Cells. To investigate responsiveness of tracheal epithelial cells to Kinin exposure, we monitored cytoplasmic calcium dynamics in *ppk4*, *ppk10>GCaMP* flies. Trachea dissected from the double vertical plate (dVP) -stage second-instar larva show moderate resting fluorescence (Fig. 4*A*). Following exposure to Kinin (10 nM), tracheal epithelial cells exhibit robust increases in fluorescence intensity, indicating increased cytoplasmic $[Ca^{2+}]_i$ levels (Fig. 4*A* and Movie S1). At this concentration of Kinin, calcium dynamics are characterized by transient spike-shaped fluctuations beginning 3.1 ± 1.85 min (n = 10). Interestingly, different tracheal regions show distinct onset timing and diverse peak fluorescence intensities (Fig. 4 *A* and *B*). We tested three different doses of Kinin (5, 10, or 20 nM) and observed dose-dependent acceleration of *ppk* cell activation timing (Fig. 4*C*).

Kinin Signaling Promotes Premature Tracheal Air-Filling. Evidence presented thus far suggests Kinin signaling is required for normal tracheal air-filling. We next investigated whether Kinin is sufficient to promote tracheal air-filling. Wild-type *Canton-S* flies (second instar) normally initiate tracheal collapse (TC) and air-filling (TA) ~20 min after the dVP (5) stage (TC = 20.6 ± 3.57; TA = 21.1 ± 3.65; n = 7) (Fig. 5*A*). Flies injected with Kinin (~100 fmol) at the dVP stage initiated TC and TA prematurely (TC = 5.0 ± 2.20; TA = 5.3 ± 2.20; n = 7). Saline injections produced no significant change in the normal latency to tracheal air-filling, albeit an increased variation in TC/TA timing (n = 6).

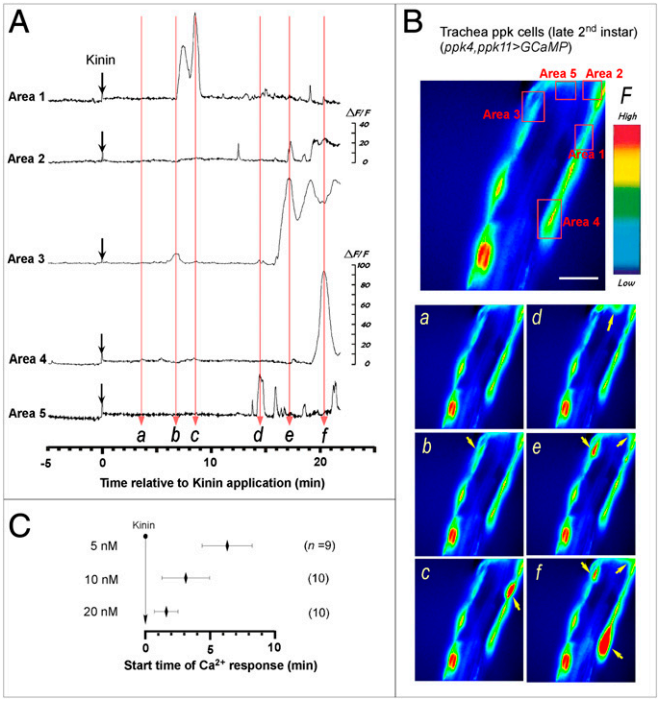

Fig. 4. Kinin-evoked Ca^{2+} dynamics in *ppk*-expressing tracheal epithelial cells. (*A*) Representative recordings of intracellular Ca^{2+} dynamics in *ppk4-GAL4, ppk11-GAL4*>GCaMP-expressing tracheal epithelial cells following exposure to Kinin (10 nM) applied at time 0 (downward black arrows). Following Kinin application, *ppk* cells showed robust Ca^{2+} oscillations after characteristic delays. (*B*) Video image shows locations of *ppk* cells where Ca^{2+}-associated fluorescence was recorded (*Upper*). (Scale bar, 25 μm.) Time-lapse video images captured during Ca^{2+} responses (*Lower*, *a–f*); timing of video image recordings in each panel labeled *a–f* are indicated by vertical, light red arrows in *A*. (*C*) Average latency of tracheal cell activation by Kinin is concentration dependent. Also see Movie S1.

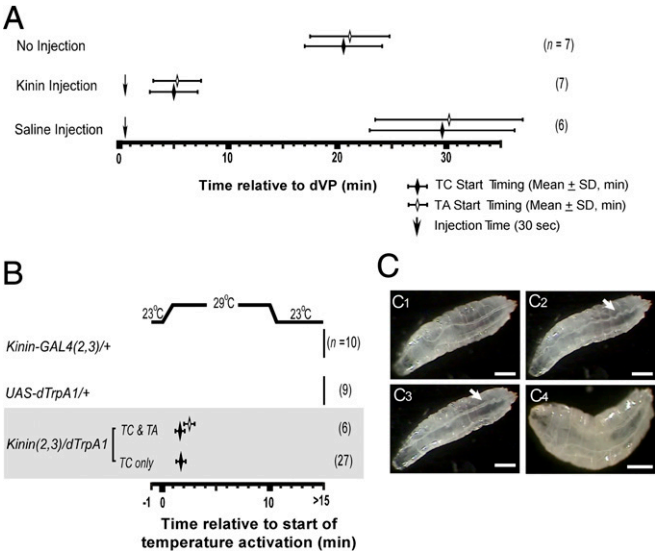

Fig. 5. Kinin induces premature tracheal air-filling in dVP larvae. (*A*) Kinin injection test. Wild-type dVP-stage second-instar larvae were used for injection tests (dVP = time 0). Under natural conditions (no injection), TC and TA occur ∼20 min after dVP. Downward arrows indicate timing of Kinin or saline injections. Kinin injection (∼100 fmol; $n = 7$) caused premature tracheal air-filling within ∼5 min in all dVP larvae. Saline injection led to delayed TC and TI with higher timing variability ($n = 6$). (*B*) dTrpA1 activation of *Kinin* neurons. Induction of TC and TA within minutes of increasing temperature from 23 °C to 29 °C in late second-instar (dVP stage) larvae [genotype: *Kinin (2, 3)>dTrpA1*]; 81% of the test animals ($n = 27$ of 33) showed TC only, while 19% ($n = 6$ out of 33) exhibited both TC and TA. Control animals exhibited no evidence of TC or TA within 15 min. (*C*) Video captures of temperature induced TC/TA in test (C_1–C_3) and control flies (C_4). (C_1) dVP-stage larva before the activation. (C_2) TC (arrow) following TrpA1 activation of Kinin neurons at 29 °C. (C_3) TA (arrow) after TC. (C_4) Control animal shows no evidence of TC or TA after temperature elevation. (Scale bars, 500 μm.) Also see Movie S2.

We then tested whether neural activation of Kinin release induces tracheal air-filling by expressing the temperature-activated dTrpA1 channel (26, 27) in *Kinin* neurons (Fig. 5*B*). Control flies at the dVP stage showed no sign of TC or TA tracheal tubules following temperature elevation. However, in *Kinin (2, 3)>dTrpA1* flies, temperature elevation induced premature TC in all animals ($n = 33$) (Fig. 5 *B* and C_2), and TA in 19% ($n = 6$ of 33) (Fig. 5 *B* and C_3). The low success rate of tracheal air-filling may result from less than complete activation of *Kinin* neurons by dTrpA1. Interestingly, among animals that showed temperature-induced TC and TA, three showed subsequent loss of gas following dTrpA1-induction of tracheal air-filling. These tracheae reinflated during natural tracheal air-filling associated with ecdysis. This observation suggests that the air-filling process is reversible and bidirectional (Movie S2).

Discussion

In *Drosophila*, developmental steps that terminate each molt through ecdysis initiation involve collapse of old trachea, air-filling of new trachea, and sequential ecdysis-related behaviors, events that occur within minutes of ETH release (5). *Kinin* neurons, among the earliest responders to ETH, promote preecdysis behavior and ecdysis-associated diuresis in *Drosophila* and *Manduca* (6–8, 28). In the present work, we tested the hypothesis that Kinin participates in the ETH signaling cascade leading to tracheal air-filling (5). Our results indicate that *Kinin* neurons indeed are targeted by ETH to promote tracheal air-filling in *Drosophila* (Figs. 1 and 6).

Kinin is a neuropeptide hormone originally discovered in association with its myotropic actions (10). Since its early characterization, it has proved to be a multifunctional hormone involved in feeding (29, 30), olfaction (31), turning behavior (32), and ecdysis behavior (7). Kinin also is a critical regulator of diuresis, water balance (28, 30, 33, 34), starvation resistance (18), cold stress recovery (35), and sugar perception (36). Tracheal air-filling and shedding of old tracheal cuticle fit the profile of previously described Kinin regulatory functions, since both muscle movement and fluid clearance are involved.

We found that ablation of *Kinin* neurons leads to a high rate of tracheal air-filling defects. Similar defects were observed upon electrical silencing of *Kinin* neurons through expression of Kir2.1 or when Kinin transcript levels are suppressed by Kinin gene-specific RNAi. Tracheal air-filling defects also were observed upon RNAi silencing of ETH receptors in *Kinin* neurons, suggesting that ETH regulates tracheal air-filling via downstream Kinin signaling.

Coincidentally, mammalian "Kinin"-like hormones function in airway clearance, including neurokinin-A (HKTDSFVGLM) and bradykinin (RPPGFSPFR) (37–39). Although sequence similarity is minimal (NSVVLGKKQRFHSWGamide) (40), it would be interesting to investigate whether these peptides may function in airway clearance at childbirth.

Further investigation into the possible regulatory role of Kinin signaling in tracheal air-filling revealed a clear deficiency phenotype in a *piggyback* insertional Kinin receptor mutant, even though severity was much lower than that resulting from *Kinin* cell ablation or electrical silencing with Kir2.1 expression. The difference in severity is attributable to the fact that Lkr^{f02594} is a hypomorphic mutant, resulting from *piggyBac* insertion into the upstream promoter of the Kinin gene (41, 42). Using precise excision of this insertion, we were able to rescue tracheal air-filling defects.

Taken together, these findings provide strong evidence that Kinin signaling is necessary for normal tracheal air-filling during the EBS. However, necessary roles of Kinin in many other functions such as water balance and feeding and high cumulative mortality associated with Kinin deficiency during development, as depicted in Fig. S2, creates uncertainty as to whether tracheal air-filling defects described here are a consequence of overall systemic debilitation. In other words, phenotypes associated with

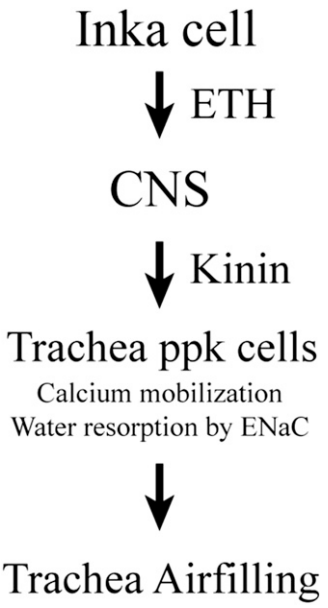

Fig. 6. Proposed model for hormonal signaling cascade leading to tracheal air-filling. Peptide ETH released from Inka cell activates Kinin neurons in the CNS to release downstream peptide Kinin hormone into the circulatory system. Kinin activation of pickpocket cells in trachea induces calcium elevation and water resorption from new trachea.

general loss of Kinin or its receptor (the Lkr^{f02594} mutant line) could compromise a variety of functions that might indirectly cause tracheal air-filling.

We addressed this issue by adopting two strategies to focus on the role of Kinin signaling specifically in tracheal epithelial cells. First, we demonstrate through tracheal-targeted knockdown of the kinin receptor using *breathless* and *pickpocket* GAL4 drivers the necessity of Kinin signaling in tracheal epithelial cells for normal tracheal air-filling. Indeed, using these cell-specific GAL4 drivers, we demonstrate that ≥80% of first-instar larvae exhibit tracheal air-filling defects. The severity of these defects resulting from tracheal epithelial cell-specific disruption of Kinin signaling (Fig. 3) is on par with failure resulting from general compromise of kinin signaling (Figs. 1 and 2). We therefore conclude that Kinin signaling in tracheal epithelial cells is both necessary and sufficient for tracheal air-filling. Second, we show sufficiency of peptide action by triggering calcium mobilization in tracheal epithelial cells and premature TC and TA in normal, healthy animals through direct Kinin exposure or Trp-A1 activation of Kinin neurons. While Radford et al. (43) reported evidence for Kinin receptors in Malpighian tubules, hindgut, brain, testis, and ovary, our report of Kinin receptors in the tracheal system is unique.

In *Drosophila* as well as mammals, DEG/ENaC expressed by *ppk* genes are required for airway clearance. In tracheal air-filling, cation flux through ENaC channels may diminish activity of the $K^+/2H^+$ antiporter, thus acidifying the tracheal lumen and eliminating bicarbonate to generate CO_2 gas (4). Our observations of loss-of-function air-filling phenotypes resulting from Kinin receptor silencing in *ppk-GAL4* lines suggests that Kinin targets *ppk* cells to facilitate tracheal air-filling. Different *ppk* genes have distinct spatial expression patterns in the larval tracheal system: *ppk4* and *ppk11* show relatively widespread expression, while other *ppk* genes are expressed in more restricted regions (12).

After demonstrating the connection between Kinin and DEG/ENaC-expressing cells, we expressed the Ca^{2+} sensor GCaMP in *ppk* cells and monitored their activation after Kinin application. We found that *ppk* cells respond to Kinin within minutes and that calcium dynamics increase in magnitude over time. Onset time accelerated from 6.3 min to 1.6 min as Kinin concentration increased from 5 to 20 nM. Robust calcium responses and dose-dependent onset timing suggests that Kinin activates tracheal epithelial cells directly by mobilizing calcium as a second messenger.

The relationship between Kinin-induced calcium mobilization in tracheal epithelial cells and the sequential events of (*i*) collapse of old trachea and (*ii*) air-filling of new trachea remains to be defined. Several possibilities can be envisioned at this point. With regard to collapse of old trachea, it is tempting to speculate that calcium mobilization in tracheal cells by Kinin promotes exocytotic release of secretory products into the tracheal lumen, disrupting luminal chitin binding proteins essential for chitin filament integrity in the taenidia. Such secretory products could cause enzymatic degradation of chitin binding proteins or in some way interfere with their binding to chitin filaments.

Regarding tracheal air-filling, Kinin could facilitate ion and fluid transport through activation of DEG/ENaC channels. Alternatively, Kinin could promote fluid transport out of the trachea through activation of anion flux to relieve the transcellular potential caused by cation transport through ENaC channels. Indeed, it is firmly established that Kinin promotes chloride flux into the lumen of Malpighian tubules through calcium mobilization in stellate cells (11, 33). In Malpighian tubules, Kinin mobilizes calcium from internal stores, triggering transcellular chloride transport into the lumen, thus facilitating transcellular fluid movement from hemolymph into the lumen (33). Interestingly, our data implicate Kinin in promotion of fluid movement in the opposite direction, from the tracheal lumen to hemolymph. Exactly how Kinin-induced calcium dynamics and ENaC-mediated Na^+ transport facilitate fluid movement out of the tracheal lumen remains a fascinating problem to pursue.

Materials and Methods

Fly Strains. All flies were raised at 25 °C on standard cornmeal-agar media under a 12-h light/dark regimen. *Kinin-GAL4 (2), Kinin-GAL4 (3)*, and *UAS-ETHR-RNAi* were described previously (7). Kinin receptor mutant flies (*PBac {WH}*Lkr^{f02594}) were obtained from Exelixis. Fly stocks from the Bloomington stock center were as follows: *UAS-rpr* (stock no. 5824), *P{Tub-PBac}* (stock no. 8285), *UAS-mCD8-GFP* (stock no. 5137), *Df(3L)Exel6105* (stock no. 7584), *Df(3L)ZN47* (stock no. 3096), *ActGFP* (stock no. 4534), *breathless-GAL4* (stock no. 8807), *repo-GAL4* (stock no. 7415), *UAS-Lkr-RNAi2* (stock no. 65934), *UAS-Lkr-RNAi3* (stock no. 25936), *Canton-S* (1), and w^{1118} (stock no. 5905). *UAS-Kinin-RNAi* (*v14091*) and *UAS-Lkr-RNAi1* (v105155) were obtained from the Vienna *Drosophila* Resource Center stock center. *NP3084-GAL4* (113094) was obtained from the *Drosophila* Genomics and Genetic Resources stock center (Kyoto). Other fly stocks used were *UAS-rpr,hid* (44), *UAS-Dicer2* (23), *UAS- Kir2.1* (45), *UAS-dTrpA1* (46). *UAS-GCaMP* (47), *ppk4-GAL*, *ppk11-GAL4* (12), *pebbled-GAL4* (7), *ELAV-GAL4* (48), and *nSyb-GAL4* (23).

Test of Defects in Tracheal Air-Filling. First-, second-, and third-instar larvae exhibiting defects in Kinin signaling were positioned in a drop of tap water on a glass slide with thin supports on both sides; a coverslip was placed over the preparation. Shapes of trachea were observed with a compound microscope. Larvae were rolled over to view detailed abnormality of tracheal tubes. The degree of defects observed was defined according to three levels: total failure, partial failure, and normal. Larvae showing a complete absence of air in the tracheal system were scored as total failure. Tracheal air-filling defects were photographed with a Sony Coolpix digital camera to illustrate morphological characteristics of tracheal defects.

Immunohistochemistry. We crossed *GAL4* transgenic flies with *UAS-mCD8-GFP* flies to produce progeny expressing GFP in *Kinin* neurons/*ppk* cells and used them for GFP immunohistochemical staining. CNS or trachea was dissected in PBS and fixed in 4% paraformaldehyde in PBS overnight at 4 °C. Tissue was washed in PBS-0.2% Triton X-100 (PBST) and incubated in 5% normal goat serum in PBST for 30 min at room temperature. Tissues were labeled incubated with mouse anti-GFP (1:1,000; Clontech, 632380), rabbit anti-Kinin (1:500), or rabbit anti-Lkr (1:100) (43) in PBST for 2 d at 4 °C. Tissues were washed with PBST and incubated with Alexa 555-conjugated goat-anti-rabbit (1:1,000; Invitrogen, A21418) or Alexa-488-conjugated goat anti-mouse (1:1,000; Invitrogen, A11001). Confocal microscopy images were acquired with either a Leica SP2 or Zeiss LSM 510 and processed in Adobe Photoshop.

***Lkr^{f02594}* Rescue Test.** For precise excision of the *piggyBac* insertion in Lkr^{f02594}, *piggyBac* transposase [w^{1118}; *P{Tub-PBac}*] flies were crossed to Lkr^{f02594}. The revertant line carrying the precise excision of *piggyback* construct was isolated from white-eyed F1 progenies, and confirmed by PCR using following primers (for relative positions of primers, see Fig. S3*A*):

F1: 5′-GACTTCGGGAGCTTTAATCGTGCG;

F2: 5′-GATATGTGCCAAAGTTGTTTCTGACTGACT;

F3: 5′-CAACGGAAGTAGTGGGCAGAACAAC;

R1: 5′-GCCACGATACTGATTCCCCCATAGA;

R2: 5′-CCCGCATCCTTGTCCTTCGC;

R3: 5′-GCATTGACAAGCACGCCTCACG.

In Vitro Ca^{2+} Imaging. In vitro Ca^{2+} imaging experiments were performed on the isolated tracheal tubes from second-instar dVP-stage larvae of *ppk4, ppk10>GCaMP*. Tracheal tubes were placed in a 500-μL fly saline bath. The test chamber consisted of a metal frame slide with 9-mm hole in the center. The bottom of the chamber was provided by a new glass coverslip, which was discarded after each experiment. We used an imaging set-up consisting of a xenon lamp and monochromator (TILL Photonics Polychrome IV) as light source and a TILL-IMAGO-QE CCD camera for image capture. The microscope (Olympus BX51WI) was equipped with a 40× water immersion NA 0.8 objective. Binning on the chip (8 × 8) was set to yield a spatial sampling rate of 1 μm per pixel (image size 172 × 130 pixels, corresponding to 172 μm and 130 μm, respectively). Images were acquired at a rate of 1 Hz. The excitation wavelength was 488 nm, and exposure time was 25 ms. Light passing an excitation

DEVELOPMENTAL BIOLOGY

filter (370–510 nm) was directed onto a 500-nm DCLP mirror followed by a 515 LP emission filter for EGFP. Continuous images (30-min duration) were acquired from each preparation and Kinin was applied into the bathing medium ~5 min after commencement of image capture. The volume of applied Kinin was 3 μL. Fluorescence intensity was calculated as $\Delta F/F$; the mean fluorescence over the entire 100 frames was taken, for each pixel, as an estimate for F. Because spontaneous calcium activity was observed in some control and of the preparations, we sampled for 5 min before Kinin application. Preparations exhibiting spontaneous activity were discarded.

Kinin Injection. We tested sufficiency of Kinin peptide for induction of tracheal air-filling by collecting *Canton-S* second-instar dVP-stage larvae and injected the peptide using a micropipette needle (~3-μm tip opening) attached to a Picospritzer (General Valve Corp.). Animals immobilized on sticky tape were injected through the lateral side of the body. Injection volumes were determined following calibration of drops under halocarbon oil, and adjusted to ~10 nL. The entire tracheal air-filling sequence was recorded with a CCD camera and analyzed later.

Induction of Tracheal Collapse and Air-Filling by dTrpA1. We activated Kinin neurons through targeted expression of the temperature-activated dTrpA1 channel. Second-instar dVP-stage larvae of *Kinin (2, 3)>dTrpA1* or w^{1118} were placed on a Peltier device for temperature regulation (Echotherm; Torrey Pines Scientific). Changes in tracheal air-filling were recorded with a CCD camera attached to video recorder.

ACKNOWLEDGMENTS. M.E.A. and D.-H.K. were supported by NIH Grant GM06730. D.-H.K. also was supported by the Basic Science Research Program through the National Research Foundation of Korea (NRF), funded by the Ministry of Education (NRF-2017R1A6A3A11027866) and Gwangju Institute of Science and Technology (GIST) Research Fellow Grant funded by the GIST in 2017. Y.-J.K. was supported by a GIST Research Institute (GRI) grant funded by the GIST in 2017.

1. Krasnow MA, Nelson WJ (2002) Tube morphogenesis. *Trends Cell Biol* 12:351.
2. Katz C, Bentur L, Elias N (2011) Clinical implication of lung fluid balance in the perinatal period. *J Perinatol* 31:230–235.
3. Eaton DC, Helms MN, Koval M, Bao HF, Jain L (2009) The contribution of epithelial sodium channels to alveolar function in health and disease. *Annu Rev Physiol* 71:403–423.
4. Förster TD, Woods HA (2013) Mechanisms of tracheal filling in insects. *Biol Rev Camb Philos Soc* 88:1–14.
5. Park Y, Filippov V, Gill SS, Adams ME (2002) Deletion of the ecdysis-triggering hormone gene leads to lethal ecdysis deficiency. *Development* 129:493–503.
6. Kim YJ, Zitnan D, Galizia CG, Cho KH, Adams ME (2006) A command chemical triggers an innate behavior by sequential activation of multiple peptidergic ensembles. *Curr Biol* 16:1395–1407.
7. Kim DH, et al. (2015) Rescheduling behavioral subunits of a fixed action pattern by genetic manipulation of peptidergic signaling. *PLoS Genet* 11:e1005513.
8. Kim YJ, et al. (2006) Central peptidergic ensembles associated with organization of an innate behavior. *Proc Natl Acad Sci USA* 103:14211–14216.
9. Hayes TK, et al. (1989) Leucokinins, a new family of ion transport stimulators and inhibitors in insect Malpighian tubules. *Life Sci* 44:1259–1266.
10. Meola SM, Clottens FL, Coast GM, Holman GM (1994) Localization of leucokinin VIII in the cockroach, Leucophaea maderae, using an antiserum directed against an achetakinin-I analog. *Neurochem Res* 19:805–814.
11. Cabrero P, et al. (2014) Chloride channels in stellate cells are essential for uniquely high secretion rates in neuropeptide-stimulated *Drosophila* diuresis. *Proc Natl Acad Sci USA* 111:14301–14306.
12. Liu L, Johnson WA, Welsh MJ (2003) *Drosophila* DEG/ENaC pickpocket genes are expressed in the tracheal system, where they may be involved in liquid clearance. *Proc Natl Acad Sci USA* 100:2128–2133.
13. Behr M, Wingen C, Wolf C, Schuh R, Hoch M (2007) Wurst is essential for airway clearance and respiratory-tube size control. *Nat Cell Biol* 9:847–853.
14. Min S, et al. (2016) Identification of a peptidergic pathway critical to satiety responses in *Drosophila*. *Curr Biol* 26:814–820.
15. de Haro M, et al. (2010) Detailed analysis of leucokinin-expressing neurons and their candidate functions in the *Drosophila* nervous system. *Cell Tissue Res* 339:321–336.
16. Herrero P, et al. (2007) Squeeze involvement in the specification of *Drosophila* leucokinergic neurons: Different regulatory mechanisms endow the same neuropeptide selection. *Mech Dev* 124:427–440.
17. Brand AH, Perrimon N (1993) Targeted gene expression as a means of altering cell fates and generating dominant phenotypes. *Development* 118:401–415.
18. Cannell E, et al. (2016) The corticotropin-releasing factor-like diuretic hormone 44 (DH44) and kinin neuropeptides modulate desiccation and starvation tolerance in *Drosophila melanogaster*. *Peptides* 80:96–107.
19. Mortimer NT, Moberg KH (2009) Regulation of *Drosophila* embryonic tracheogenesis by dVHL and hypoxia. *Dev Biol* 329:294–305.
20. de Miguel C, Linsler F, Casanova J, Franch-Marro X (2016) Genetic basis for the evolution of organ morphogenesis: The case of spalt and cut in the development of insect trachea. *Development* 143:3615–3622.
21. Mukherjee T, Choi I, Banerjee U (2012) Genetic analysis of fibroblast growth factor signaling in the *Drosophila* eye. *G3 (Bethesda)* 2:23–28.
22. Berger C, Renner S, Lüer K, Technau GM (2007) The commonly used marker ELAV is transiently expressed in neuroblasts and glial cells in the *Drosophila* embryonic CNS. *Dev Dyn* 236:3562–3568.
23. Lee KM, et al. (2015) A neuronal pathway that controls sperm ejection and storage in female *Drosophila*. *Curr Biol* 25:790–797.
24. Nehme NT, et al. (2007) A model of bacterial intestinal infections in *Drosophila melanogaster*. *PLoS Pathog* 3:e173.
25. Toczyłowska-Mamińska R, Dołowy K (2012) Ion transporting proteins of human bronchial epithelium. *J Cell Biochem* 113:426–432.
26. Pulver SR, Pashkovski SL, Hornstein NJ, Garrity PA, Griffith LC (2009) Temporal dynamics of neuronal activation by channelrhodopsin-2 and TRPA1 determine behavioral output in *Drosophila* larvae. *J Neurophysiol* 101:3075–3088.
27. Rosenzweig M, et al. (2005) The *Drosophila* ortholog of vertebrate TRPA1 regulates thermotaxis. *Genes Dev* 19:419–424.
28. Diao F, et al. (2016) The splice isoforms of the *Drosophila* ecdysis triggering hormone receptor have developmentally distinct roles. *Genetics* 202:175–189.
29. Al-Anzi B, et al. (2010) The leucokinin pathway and its neurons regulate meal size in *Drosophila*. *Curr Biol* 20:969–978.
30. Liu Y, Luo J, Carlsson MA, Nässel DR (2015) Serotonin and insulin-like peptides modulate leucokinin-producing neurons that affect feeding and water homeostasis in *Drosophila*. *J Comp Neurol* 523:1840–1863.
31. López-Arias B, Dorado B, Herrero P (2011) Blockade of the release of the neuropeptide leucokinin to determine its possible functions in fly behavior: Chemoreception assays. *Peptides* 32:545–552.
32. Okusawa S, Kohsaka H, Nose A (2014) Serotonin and downstream leucokinin neurons modulate larval turning behavior in *Drosophila*. *J Neurosci* 34:2544–2558.
33. Halberg KA, Terhzaz S, Cabrero P, Davies SA, Dow JA (2015) Tracing the evolutionary origins of insect renal function. *Nat Commun* 6:6800.
34. Yu MJ, Beyenbach KW (2002) Leucokinin activates Ca(2+)-dependent signal pathway in principal cells of *Aedes aegypti* Malpighian tubules. *Am J Physiol Renal Physiol* 283: F499–F508.
35. Terhzaz S, et al. (July 17, 2017) Renal neuroendocrine control of desiccation and cold tolerance by *Drosophila suzukii*. *Pest Manag Sci*, 10.1002/ps.4663.
36. Kwon H, et al. (2016) Leucokinin mimetic elicits aversive behavior in mosquito *Aedes aegypti* (L.) and inhibits the sugar taste neuron. *Proc Natl Acad Sci USA* 113:6880–6885.
37. Canning BJ (2006) Neurokinin3 receptor regulation of the airways. *Vascul Pharmacol* 45:227–234.
38. Farmer SG (1991) Role of kinins in airway diseases. *Immunopharmacology* 22:1–20.
39. Advenier C, Naline E, Drapeau G, Regoli D (1987) Relative potencies of neurokinins in Guinea pig trachea and human bronchus. *Eur J Pharmacol* 139:133–137.
40. Torfs P, et al. (1999) The kinin peptide family in invertebrates. *Ann N Y Acad Sci* 897:361–373.
41. Elick TA, Bauser CA, Fraser MJ (1996) Excision of the piggyBac transposable element in vitro is a precise event that is enhanced by the expression of its encoded transposase. *Genetica* 98:33–41.
42. Fraser MJ, Ciszczon T, Elick T, Bauser C (1996) Precise excision of TTAA-specific lepidopteran transposons piggyBac (IFP2) and tagalong (TFP3) from the baculovirus genome in cell lines from two species of Lepidoptera. *Insect Mol Biol* 5:141–151.
43. Radford JC, Davies SA, Dow JA (2002) Systematic G-protein-coupled receptor analysis in *Drosophila melanogaster* identifies a leucokinin receptor with novel roles. *J Biol Chem* 277:38810–38817.
44. Yoo SJ, et al. (2002) Hid, Rpr and Grim negatively regulate DIAP1 levels through distinct mechanisms. *Nat Cell Biol* 4:416–424.
45. Paradis S, Sweeney ST, Davis GW (2001) Homeostatic control of presynaptic release is triggered by postsynaptic membrane depolarization. *Neuron* 30:737–749, and erratum (2001) 31:167.
46. Kang K, et al. (2010) Analysis of *Drosophila* TRPA1 reveals an ancient origin for human chemical nociception. *Nature* 464:597–600.
47. Wang JW, Wong AM, Flores J, Vosshall LB, Axel R (2003) Two-photon calcium imaging reveals an odor-evoked map of activity in the fly brain. *Cell* 112:271–282.
48. Oh Y, et al. (2014) A homeostatic sleep-stabilizing pathway in *Drosophila* composed of the sex peptide receptor and its ligand, the myoinhibitory peptide. *PLoS Biol* 12:e1001974.